Key Points:
- Snow contributed 7.5–9.7% (by mass) in a thinner Arctic sea ice pack north of Svalbard in winter and spring
- Second-year ice contained significantly more snow than first-year ice (12.7–16.3% versus 3.3–4.4%)
- With thinner Arctic sea ice, the snow:ice thickness ratio is similar than in the Antarctic, increasing the potential for snow-ice formation

Supporting Information:
- Supporting Information S1

Correspondence to:
M. Granskog,
mats.granskog@npolar.no

Snow contribution to first-year and second-year Arctic sea ice mass balance north of Svalbard

Mats A. Granskog[1] [iD], Anja Rösel[1] [iD], Paul A. Dodd[1] [iD], Dmitry Divine[1], Sebastian Gerland[1], Tõnu Martma[2] [iD], and Melanie J. Leng[3] [iD]

[1]Norwegian Polar Institute, Fram Centre, Tromsø, Norway, [2]Department of Geology, Tallinn University of Technology, Tallinn, Estonia, [3]NERC Isotope Geosciences Facilities, British Geological Survey, Keyworth, UK

Abstract The salinity and water oxygen isotope composition (δ^{18}O) of 29 first-year (FYI) and second-year (SYI) Arctic sea ice cores (total length 32.0 m) from the drifting ice pack north of Svalbard were examined to quantify the contribution of snow to sea ice mass. Five cores (total length 6.4 m) were analyzed for their structural composition, showing variable contribution of 10–30% by granular ice. In these cores, snow had been entrained in 6–28% of the total ice thickness. We found evidence of snow contribution in about three quarters of the sea ice cores, when surface granular layers had very low δ^{18}O values. Snow contributed 7.5–9.7% to sea ice mass balance on average (including also cores with no snow) based on δ^{18}O mass balance calculations. In SYI cores, snow fraction by mass (12.7–16.3%) was much higher than in FYI cores (3.3–4.4%), while the bulk salinity of FYI (4.9) was distinctively higher than for SYI (2.7). We conclude that oxygen isotopes and salinity profiles can give information on the age of the ice and enables distinction between FYI and SYI (or older) ice in the area north of Svalbard.

Plain Language Summary The role of snow in sea ice mass balance is largely two fold. Firstly, it can slow down growth and melt due to its high insulation and high reflectance, but secondly it can actually contribute to sea ice growth if the snow cover is turned into ice. The latter is largely a consequence of high mass of snow on top of sea ice that can push the surface of the sea ice below sea level and seawater can flood the ice. This mixture of seawater and snow can then freeze and add to the growth of sea ice. This is very typical in the Antarctic but not believed to be so important in the Arctic. In this work we show, for the first time, that snow actually contributes significantly to the growth of Arctic sea ice. This is likely a consequence of the thinning of the Arctic sea ice. The conditions in the Arctic, with thinner and more seasonal ice thus resemble the ice pack in the Antarctic. Studies on the role of snow in the Arctic are critical to be able to understand the ongoing changes of the Arctic sea ice pack.

1. Introduction

The snow cover on sea ice is a critical factor affecting the growth and decay of sea ice, by virtue of it's strong insulative properties and its high albedo and their role in sea ice evolution [e.g., *Massom et al.*, 2001; *Sturm and Massom*, 2010]. Given the importance of the snow cover, surprisingly little is known about snow depth distribution on Arctic sea ice. *Warren et al.*'s [1999] compilation of data is still widely used, while recent data is limited to the western Arctic [*Kurtz and Farrell*, 2011; *Webster et al.*, 2014]. But essentially, the snow cover on Arctic sea ice is one of the key gaps in our knowledge [e.g., *Meier et al.*, 2014].

Apart from moderating the growth and melt of sea ice, due to its strong insulative properties and high albedo, snow can directly contribute to the mass balance of sea ice through two main mechanisms, namely snow-ice and superimposed ice formation. Snow-ice forms when the ice surface is depressed below sea level (i.e., sea ice has a negative freeboard), and seawater floods onto the ice and a layer composed of a mixture of snow and sea water (slush) is formed. The "rule of thumb" is that when the snow depth on sea ice exceeds one third of the sea ice thickness (i.e., the snow:ice thickness ratio is >1/3), the sea ice surface can be pushed below sea level [e.g., *Sturm and Massom*, 2010]. However, ice deformation may also result in parts of ice floes being submerged below sea level [*Massom et al.*, 2001]. Flooding is also dependent on open pathways for seawater to flood the ice, i.e., either a permeable ice cover or other pathways such as cracks or

lateral flooding of floes. The slush formed by flooding of seawater at the bottom of the snow pack can freeze, and form snow-ice on top of the existing sea-ice cover [e.g., *Haas et al.*, 2001], despite the presence of a thick insulating snow cover that otherwise would limit thermodynamic ice growth [*Sturm and Massom*, 2010]. Superimposed ice, on the other hand, is formed when snow meltwater refreezes [e.g., *Kawamura et al.*, 1997] at the snow/ice interface, when the ice is colder than the freezing temperature of freshwater [*Nicolaus et al.*, 2003]. Hence superimposed ice is different from both sea ice and snow-ice because it consists only of freshwater ice when it is formed.

To date, snow-ice has been considered to be a predominantly Antarctic process [e.g., *Sturm and Massom*, 2010]. There, flooding and snow-ice formation is a widespread process, in all seasons and regions [e.g., *Lange et al.*, 1990; *Eicken et al.*, 1994; *Jeffries et al.*, 1994, 1997, 2001; *Kawamura et al.*, 1997; *Eicken*, 1998; *Haas et al.*, 2001]. Estimates of snow-ice as a fraction of total sea ice mass range from 7% [*Lange et al.*, 1990] to almost 40% [*Jeffries et al.*, 2001], depending on region (and season), while the fraction of snow itself to the mass of sea ice (i.e., snow fraction by mass) can be up to 14–16% [*Jeffries et al.*, 1997].

Sturm and Massom [2010] suggested that in the central Arctic snow on sea ice seldom reaches a mass that could result in flooding although this may change with climate change. It has been considered that the thicker Arctic ice cover with less snow than in the Antarctic results in a lesser role of snow in Arctic sea ice mass balance and has thus spurred less interest in studies of snow contribution to mass balance [e.g., *Fichefet and Maqueda*, 1999]. In one of the few studies on the topic from the high-Arctic, *Kawamura et al.* [2001b] show negligible contribution of snow to sea-ice mass balance for landfast sea ice in the Baffin Bay North Water Polynya region. In contrast, snow has been shown to contribute significantly in Northern Hemisphere marginal seas and fjords, with thinner ice and more temperate conditions, snow fraction by mass was estimated at 8% for pack ice in the Sea of Okhotsk [*Ukita et al.*, 2000], about 8% on landfast ice in Kongsfjorden (Svalbard) [*Nicolaus et al.*, 2003] and typically as much as 10–20% for landfast ice in the northern Baltic Sea [*Kawamura et al.*, 2001a; *Granskog et al.*, 2003, 2006; *Uusikivi et al.*, 2011]. For very thin landfast ice covers in the Baltic Sea, values up to 35% have been reported [*Granskog et al.*, 2004].

Due to both the thinning of the Arctic sea ice pack [e.g., *Lindsay and Schweiger*, 2015] and projected increases in precipitation in winter [e.g., *Bintanja and Selten*, 2014], the potential for snow-ice formation is possibly increased due to a change in the snow:ice thickness ratio. Considering that ice thickness in the Arctic basin has already decreased dramatically, e.g., *Lindsay and Schweiger* [2015] report on annual mean thickness of only 1.25 m in 2012 (compared to >3 m in late 1970s), with a typical snow depth of 0.3–0.4 m [*Warren et al.*, 1999], the snow:ice thickness ratio is approaching typical Antarctic conditions. However, whether the snow will fall in the open ocean or on sea ice is under debate [*Hezel et al.*, 2013]. Nevertheless, a thinner ice cover will be more susceptible to snow-ice formation, especially in autumn and early winter while the ice is thin [cf. *Sturm and Massom*, 2010]. There have been reports of thinner snow cover on FYI in the western Arctic [*Kurtz and Farrell*, 2011; *Webster et al.*, 2014]. However, it remains unknown whether this is simply because of less snow accumulated on the ice, more snow being incorporated into the ice cover due to snow-ice or superimposed ice formation [cf. *Jeffries et al.*, 2001], or a combination of both. There are virtually no reports on the contribution of snow to sea ice mass in the central Arctic pack ice that can be used to assess whether this has changed.

Recent work on pack ice north of Svalbard with ice mass balance (IMB) buoys, that can detect both bottom and surface ice growth/melt using thermal resistivity measurements, showed episodic flooding and potential snow-ice formation events in winter [*Provost et al.*, 2017]. Thick snow cover in the region (0.5 m on average) and an ice pack with modal ice thicknesses <1.3 m [*Rösel et al.*, 2016a,2016b; *King et al.*, 2016] resulted in flooding and snow-ice formation during floe breakup events and when basal ice melt resulted in negative freeboards for level ice near the ice edge. Observations by *Provost et al.* [2017] resemble the observations reported by *Tucker et al.* [1991] of flooding near the ice edge further south in Fram Strait. Recent studies north of Svalbard also indicate heavy snow loads and frequent occurrence of negative freeboards in spring [*Haapala et al.*, 2013; *Nomura et al.*, 2013], in support of the potential for snow-ice formation. This is quite opposite to the reported thinning of the snow cover on FYI for the western Arctic [*Kurtz and Farrell*, 2011; *Webster et al.*, 2014]. Thus, there might be critical regional patterns in snow depth on Arctic sea ice that we are not well aware of due to lack of observational data.
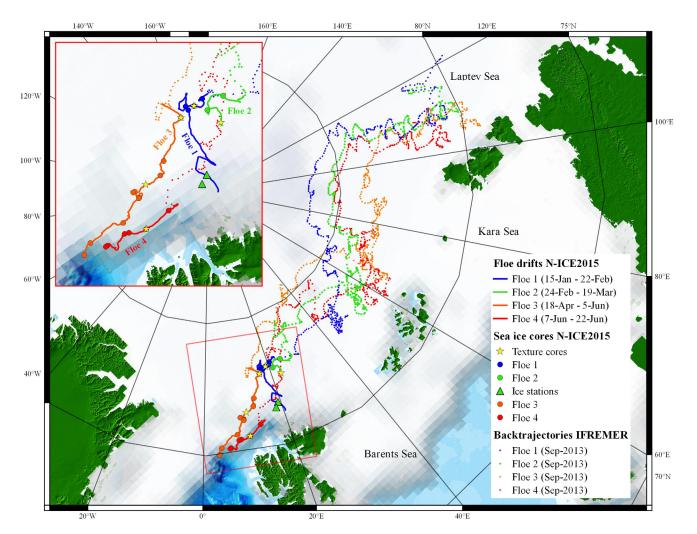
Figure 1. Location of N-ICE2015 floe drifts and calculated back trajectories (i.e., the origin) of the ice floes until September 2013 (Itkin et al., submitted manuscript, 2017). Insert shows in detail where ice cores were collected during each floe drift or at ice stations. Shading shows ice concentration in May 2015 from *Cavalieri et al.* [1996].

Motivated by the lack of information on actual snow contribution to Arctic sea ice mass balance, we collected sea ice cores during the Norwegian young sea ICE (N-ICE2015) expedition in pack ice at the western end of the Transpolar Drift System north of Svalbard [*Granskog et al.*, 2016]. Here we report on results from the first water oxygen isotopic analyses of sea ice cores in the region, that can be used to quantify the contribution of snow [*Jeffries et al.*, 1994, 1997, 2001]. While *Provost et al.* [2017] specifically report on direct observations of sea-ice flooding and potential for snow-ice formation from IMBs near the ice edge, we show that snow contributed significantly to the mass balance of sea ice over a larger region in the Nansen Basin in winter and spring 2015.

2. Material and Methods

2.1. Sampling and Analyses

Sea ice cores were collected during N-ICE2015 expedition [*Granskog et al.*, 2016]. The campaign took place in the area north of Svalbard, between 80°N and 83°N and in January–June 2015. During the experiment, research camps were established on four different ice floes using research vessel Lance as base (Figure 1). The floes drifted with the ice pack while measurements were undertaken in the vicinity of the ship [see *Granskog et al.*, 2016]. The origin and age of the ice in the study region was examined by sea ice back trajectories [*Girard-Ardhuin and Ezraty*, 2012] which placed the origin of the oldest ice region to the Laptev Sea

Table 1. Sea Ice Cores Collected and Analyzed for Water Oxygen Isotopic ($\delta^{18}O$) Composition During the N-ICE2015 Campaign

Date	Floe	Site	Latitude (°N)	Longitude (°E)	Structure	Ice Thickness (cm)	Snow Depth (cm)	Freeboard (cm)	Bulk Salinity
26 Jan 2015[a]	1	Crossroads	83.049	18.989	Yes	134	46	−1	1.6
18 Mar 2015[a]	2	Supersite	82.615	22.772	Yes	125	45	−3	2.1
22 Apr 2015[a]	3	Main coring site	82.848	16.576	Yes	142	50	1	2.3
10 May 2015[a]	3	Secondary site	81.533	10.705	Yes	139	11	14	4.4
13 Jun 2015[a]	4	Site 2	80.625	10.707	Yes	108	28	−2	5.4
22 Jan 2015	1	Tracer site 1	83.165	20.570	n/a	89	n/a	0	5.2
26 Jan 2015	1	Crossroads	83.049	18.989	n/a	134	45	−1	5.4
29 Jan 2015	1	Tracer site 2	83.063	17.582	n/a	110	n/a	−1	2.1
6 Feb 2015	1	Crossroads	82.983	17.933	n/a	129	50	2	2.6
5 Mar 2015	2	Supersite	83.142	24.127	n/a	100	24	−2	4.8
12 Mar 2015	2	Supersite	82.920	21.410	n/a	69	37	−3	5.3
21 Mar 2015	n/a	Ice station	81.623	19.250	n/a	74	9	3	7.0
23 Mar 2015	n/a	Ice station 2	81.452	18.421	n/a	104	34	2	3.6
22 Apr 2015	3	Main coring site	82.848	16.576	n/a	138	50	1	2.4
30 Apr 2015	3	Main coring site	82.000	13.361	n/a	140	47	2	3.0
7 May 2015	3	Main Coring site	81.709	12.782	n/a	141	56	0	2.4
13 May 2015	3	CO$_2$ site	81.371	9.014	n/a	127	26.5	3.5	5.4
21 May 2015	3	Main coring site	81.263	9.809	n/a	136	43	1	3.3
21 May 2015	3	Secondary site	81.253	9.779	n/a	143	26	1	5.8
28 May 2015	3	Main coring site	80.744	7.809	n/a	126	41	0	2.4
28 May 2015	3	Secondary site	n/a	n/a	n/a	134	23	0	5.3
4 Jun 2015	3	Main coring site	80.286	3.959	n/a	124	n/a	0	2.5
5 Jun 2015	3	Secondary site	80.026	3.404	n/a	108	20	1	4.9
11 Jun 2015	4	Site 1	80.983	13.634	n/a	64	4	2	6.4
13 Jun 2015	4	Site 2	80.625	10.707	n/a	109	28	−2	5.3
15 Jun 2015	4	Site 3	80.547	8.559	n/a	89	10	n/a	5.0
17 Jun 2015	4	Site 2	80.522	8.042	n/a	88	17	−6	4.8
21 Jun 2015	4	Floe NB 1	80.263	6.018	n/a	98	2	10	4.1
21 Jun 2015	4	Floe NB 2	80.239	5.846	n/a	96	1	6	4.5

[a]These cores had a structural analysis done.

region in fall 2013, thus the oldest ice in the study area was SYI [*Itkin et al.*, 2017]. The floes were representative of the conditions in the study area in terms of ice and snow thickness based on regional-scale airborne measurements [*Rösel et al.*, 2016a,2016b; *King et al.*, 2016]. Snow depths were typically 0.3-0.5m , with ice thickness in the range of 1.0–1.5 m in the study area.

Details of the snow and ice conditions and the 29 cores collected that were analyzed for water oxygen isotope composition during the course of the campaign are given in Table 1 . The location where the ice cores were sampled are indicated in Figure 1.

On Floe 1, same site "Crossroads" was visited twice, but to avoid effects of possible flooding after coring, subsequent cores were not collected in exactly the same spot (but within 50 m radius). One of the times a second core was collected for structural analysis (Table 1). Two other sites were also visited once on Floe 1 (Table 1). Thus, these cores give a good spatial coverage of Floe 1. Floe 1 was over 100 km from the ice edge when the ice cores were collected.

On Floe 2, four subsequent cores were collected in the same area of the floe ("Supersite"), but to avoid possible flooding due to negative freeboards (Table 1) subsequent cores were far apart (in the end within an area of 100 by 100 m), and only one of the cores was analyzed for structural composition (Table 1). These also represent a spatial sampling of the floe. Floe 2 was >150 km from the ice edge at all times. On transit to Longyearbyen, after Floe 2 broke up, two random ice floes were sampled, on 21 and 23 March (Table 1).

On Floe 3, three sites were sampled, with the "main site" and the "secondary site" being visited several times (Table 1). The two sites were about 800 m apart on the larger floe. Within each site, the distance between subsequent cores was on the order of 25–30 m, to avoid possible effects of flooding. A third site was sampled coincident with CO$_2$ flux measurements. Also, here the sampling represents as much spatial variability as it does temporal variability. The distance of Floe 3 ranged from >150 km to being at the ice edge, although the main floe had not broken up by the time the last ice cores were collected.

On Floe 4, several sites were sampled (Table 1), some of them after the larger floe had broken up into smaller floes (21 June, Table 1). Again, subsequent cores ("Site 2") were taken far apart to avoid possible effects from flooding. These cores represent a good sample of spatial variability on Floe 4. On 13 June, two adjacent cores were collected at "Site 2," one was melted immediately and second was collected for structural analysis (Table 1).

Sea ice cores were collected with Kovacs Enterprises MARK type coring systems using an electric drill or petrol engine. Each structural core was immediately placed in plastic tubing and transferred to a freezer onboard the ship. In winter, the air temperatures were low, and cores froze already before being transported to the ship for storage.

Cores acquired for salinity and oxygen isotope measurements only were immediately cut into about 10 cm segments, placed in airtight containers and melted at room temperature. Melted samples were mixed carefully before subsamples were taken for salinity and oxygen isotope ratio (δ^{18}O) measurements. Salinity samples were put into glass bottles and salinity measured onboard using a Guildline 8410A salinometer. For δ^{18}O samples, melted ice water was filled into 40 mL glass vials, without headspace, closed tightly and sealed with parafilm. Seawater samples were collected for reference (see below) throughout the N-ICE2015 campaign into 40 mL glass vials and sealed with Parafilm (P. A. Dodd, unpublished data, 2015) and salinity was measured as above. Samples for δ^{18}O from Floe 1 (sea ice, snow, and seawater) were measured at G.G. Hatch Stable Isotope Laboratory at the University of Ottawa (Canada) using a Thermo Delta Plus XP system [e.g., *Dodd et al.*, 2012]. The analytical precision was determined as 0.05‰. Samples collected from Floes 2, 3, and 4 were analyzed at the National Environment Research Council Isotope Geosciences Facility at the British Geological Survey (Keyworth, UK) using an Isoprime 100 mass spectrometer. Analytical reproducibility was <0.05‰ based on duplicate analyses.

On a number of occasions, at least once from each floe, ice cores were collected for structural analyses (Table 1). These five cores were either processed in the freezer container onboard the ship or back at the freezer lab at the Norwegian Polar Institute in Tromsø. Thick and thin sections were prepared as described in *Lange* [1988] to quantify the amount of granular and columnar ice, which in combination with the δ^{18}O composition provides information on the growth conditions of the ice [*Lange*, 1988]. From the sections (usually about 10 cm) subsamples were cut and placed in a zip-lock bag, and most of the air in the bags was removed from the bags and thereafter samples were melted at room temperature. Salinity was measured directly with a WTW Cond 3110 probe (WTW Wissenschaftlich-Technische Werkstätten GmbH, Weilheim, Germany), and a 15 mL HDPE bottle was filled completely and sealed with parafilm. From these samples, δ^{18}O was measured with a Picarro L2120-i water isotope analyzer (cavity ring-down spectroscopy technology) with a high-precision A0211 vaporizer at the Tallinn Technical University. Reproducibility of δ^{18}O measurements was ±0.1‰ and analytical precision ±0.1‰. All isotope measurements were calibrated to Vienna standard mean ocean water (V-SMOW).

2.2. Analysis of Snow Fraction

Here we distinguish snow-ice and superimposed ice from sea ice formed from seawater alone based on their different δ^{18}O signatures [e.g., *Jeffries et al.*, 1994, 1997; *Granskog et al.*, 2003]. To derive the fraction of snow (by mass), we chose to use the method established by *Jeffries et al.* [1994], developed from work by *Lange et al.* [1990], as this has been widely used across different sea ice environs [e.g., *Jeffries et al.*, 1994, 1997, 2001; *Kawamura et al.*, 2001a; *Granskog et al.*, 2003, 2004]. Thus, our results are directly comparable to the bulk of literature available on snow contribution to sea ice mass. The fraction of snow f_s in a sea ice sample is calculated as follows [*Jeffries et al.*, 1994]:

$$f_s = \frac{\delta - \delta_{ref}}{\delta_{snow} - \delta_{ref}}$$

where δ is the measured δ^{18}O value, δ_{snow} the value for snow, and δ_{ref} is a reference value relative to which the fraction of snow is computed against. A number of approaches have been taken to define the value of δ_{ref} [cf. *Jeffries et al.*, 1997; *Granskog et al.*, 2003].

The δ^{18}O value for snow δ_{snow} is based on observations of the snow pack on the sea ice during the N-ICE2015 campaign, with $\delta_{snow} = -16.8 \pm 2.4$‰ (mean ± standard deviation, n = 10). These are averages from samples covering the whole snow cover. This is in fair agreement with freshly collected snow

precipitation during N-ICE2015 with $\delta^{18}O$ values of $-17 \pm 6‰$ (n = 10; range -11 to $-30‰$). Observations of $\delta^{18}O$ in solid precipitation from Ny-Ålesund (Svalbard) of $-13 \pm 5‰$ (n = 63), a more temperate Arctic location south of the drift area (D. Divine, unpublished data, 2016), also yield nearly similar values. f_s values above unity are set to a value of 1 [cf. *Granskog et al.*, 2003]. As the f_s estimate is most sensitive to the δ_{snow} value [*Jeffries et al.*, 2001], we have followed the approach by *Jeffries et al.* [2001] and used a range of snow values to allow for the possible variability of snow properties. The f_s and F values were thus calculated with three different δ_{snow} values: $-14.4‰$, $-16.8‰$, and $-19.2‰$. According to *Jeffries et al.* [2001], these f_s values are probably conservative estimates because some of the snow incorporated into the slush dissolves and is transported during the freezing of the snow-ice layer with the brine that flows into the underlying ice.

For this work, we use three different δ_{ref} values, depending on whether structural information is available or not (see below). One approach is to use the value for seawater as δ_{ref} [cf. *Jeffries et al.*, 1997; *Granskog et al.*, 2003], which is based on our observations of surface waters in the N-ICE2015 study region north of 82°N of, with $\delta_{sw} = -0.1 \pm 0.1‰$ (n = 21) and gives a lower bound for the contribution of snow [cf. *Jeffries et al.*, 1997]. Another approach is to use the values of columnar ice δ_{coli} in a core which we can use for cores with structural information. Using values for columnar ice, δ_{coli} in each core can be considered to provide an upper limit for f_s as it takes into account some of the fractionation [cf. *Toyota et al.*, 2013] occurring during freezing of seawater [cf. *Granskog et al.*, 2003, Criterion 3]. For the cores with only salinity and $\delta^{18}O$ data, we estimate the bottom ice value δ_{boti} from the profile data (see below).

The total snow fraction F (by mass) in an ice core was obtained following *Granskog et al.* [2003] by summation of all contributions from sections in an ice core that were identified as having a contribution from snow using the above (isotopic) criteria:

$$F = \frac{\sum f_s \times h_i}{\sum h_i}$$

where f_s is the snow fraction of an individual layer (see above) with thickness h_i. Subscripts of F (*sw, coli*, or *boti*) indicate which δ_{ref} value was used to calculate f_s (see above).

3. Results and Discussion

3.1. Texture, Salinity, and $\delta^{18}O$ Profiles

The five cores with structural data (Table 1 and Figure 2 and supporting information Figures S1–S5) show a variable contribution of granular ice from 10 to 30% of the total length of the cores, comparable to earlier studies in the Arctic basin [*Eicken et al.*, 1995; *Tucker et al.*, 1999; *Perovich et al.*, 2009]. Further direct intercomparison is hampered by the different classification schemes used by different investigators [cf. *Tucker et al.*, 1999], and in our case, the limited amount of data to make any further conclusions.

Granular ice was present almost exclusively at the surface and the surface granular layers had lower $\delta^{18}O$ compared to the columnar ice at the bottom of the cores. The low $\delta^{18}O$ is indicative of contribution from snow [e.g., *Lange et al.*, 1990; *Jeffries et al.*, 1994, 1997] in these ice layers (Figures 2b and 3 and supporting information Figures S1–S5). Defining granular ice layers with $\delta^{18}O$ values $<0‰$ as snow-ice [cf. *Jeffries et al.*, 1994], the contribution of snow-ice layers to total ice thickness in the five cores ranged from 6 to 28% (with a mean of 20%, using the *absolute* method by *Jeffries* [1997]). This is somewhat lower than for landfast sea ice in the Baltic Sea [*Granskog et al.*, 2003] or pack ice in the Ross, Amundsen, and Bellingshausen Seas [*Jeffries et al.*, 2001]. In our 29 ice cores, snow-ice was as ubiquitous as found by *Jeffries et al.* [2001] in the Antarctic.

We can distinguish two types of salinity-$\delta^{18}O$ profiles in our cores. The first has a very homogeneous isotopic composition and salinity below the low-$\delta^{18}O$ surface layer, and is indicative of FYI due to its relatively high salinity (Figure 3b and supporting information Figures S4 and S5). The second type of profile is identical to those in Figure 3a (see also Figure 2 and supporting information Figures S1 and S2), with two distinctly different layers in the bottom half of the core.

We suggest that for the second type, the upper of these two layers in the bottom part of the cores (e.g., Figure 3a and supporting information Figures S1 and S2, indicated by solid black line in Figure 3a) is formed when the ice has grown rapidly (when thin) and in waters with lower $\delta^{18}O$ values and possibly lower
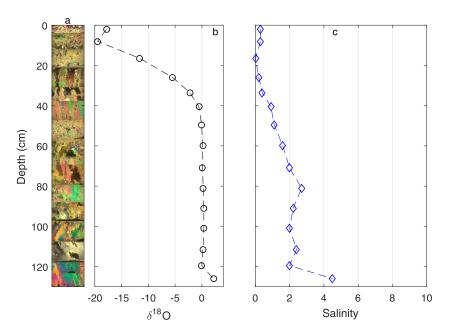
Figure 2. (a) Structural composition from thin sections under polarized light, and profiles of (b) $\delta^{18}O$ and (c) salinity from an ice core collected on 26 January at site "Crossroads" on Floe 1 (Table 1). Also, see supporting information Figures S1–S5.

salinity, and has subsequently been desalinated during summer melt. Desalination affects salinity, but has less impact on $\delta^{18}O$ as its signal comes primarily from the solid ice fraction of the ice cover. We surmise the bottommost layer with higher salinity and $\delta^{18}O$ (Figure 3a and supporting information Figures S1 and S2) is likely formed more recently, during the second winter in the more Atlantic influenced waters of the N-ICE2015 study region. Because this bottommost layer has similar salinity and $\delta^{18}O$ characteristics to the FYI cores (Figures 3a and 3b and supporting information Figures S4 and S5). Surface waters in the N-ICE2015 region in winter had an absolute salinity of 34.30 ± 0.05 (n = 21) and $\delta^{18}O$ values of $-0.1 \pm 0.1‰$ (n = 21).
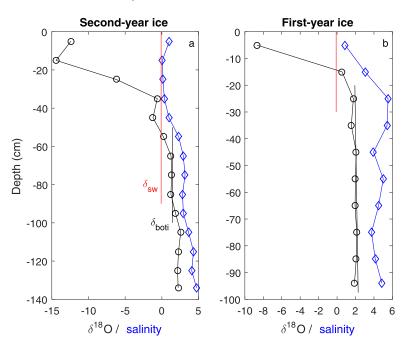

Figure 3. Salinity and $\delta^{18}O$ profiles for ice cores collected on (a) 22 April on Floe 3 and (b) 21 June on Floe 4. Without structural information, we estimate the bottom ice $\delta^{18}O$ value δ_{boti} (see text). (a) For the second-year ice core, the value for bottom ice is the average of the layer with constant values with depth right below the surface layer and indicated by the solid black line. (b) For first-year ice, there is typically one rather homogeneous layer that is used to derive δ_{boti}. The second reference used, the value for seawater δ_{sw} value ($-0.1‰$), is shown with a solid red line. Note the different axis scales in the two panels.

Table 2. Summary of δ_{ref} Values, Namely δ_{boti} and δ_{coli} in the Ice Cores and Fraction of Snow (by Mass) F in Each Core Based on Use of Different δ_{ref} Values and the Mean Value for Snow ($\delta_{snow} = -16.8‰$)[a]

Date	Floe	Site	Ice Type	δ_{boti} (‰)	δ_{coli} (‰)	F_{sw}	F_{boti}	F_{coli}
26 Jan 2015[b]	1	Crossroads	SYI	n/a	0.10	0.18	n/a	0.18
18 Mar 2015[b]	2	Supersite	SYI	n/a	1.20	0.06	n/a	0.08
22 Apr 2015[b]	3	Main site	SYI	n/a	1.30	0.13	n/a	0.14
10 May 2015[b]	3	Secondary site	FYI	n/a	2.30	0.01	n/a	0.01
13 Jun 2015[b]	4	Site 2	FYI	n/a	2.40	0.11	n/a	0.13
22 Jan 2015	1	Tracer site 1	FYI	2.17	n/a	0.01	0.04	n/a
26 Jan 2015	1	Crossroads	SYI	0.32	n/a	0.18	0.18	n/a
29 Jan 2015	1	Tracer site 2	FYI	2.16	n/a	0.00	0.00	n/a
6 Feb 2015	1	Crossroads	SYI	0.50	n/a	0.14	0.15	n/a
5 Mar 2015	2	Supersite	FYI	2.24	n/a	0.11	0.14	n/a
12 Mar 2015	2	Supersite	FYI	2.11	n/a	0.00	0.00	n/a
21 Mar 2015	n/a	Ice station	FYI	1.60	n/a	0.00	0.00	n/a
23 Mar 2015	n/a	Ice station 2	SYI	1.65	n/a	0.13	0.15	n/a
22 Apr 2015	3	Main coring site	SYI	1.42	n/a	0.15	0.17	n/a
30 Apr 2015	3	Main coring site	SYI	1.61	n/a	0.14	0.15	n/a
7 May 2015	3	Main coring site	SYI	1.76	n/a	0.10	0.10	n/a
13 May 2015	3	CO_2 site	FYI	2.14	n/a	0.00	0.00	n/a
21 May 2015	3	Main coring site	SYI	1.82	n/a	0.16	0.18	n/a
21 May 2015	3	Secondary site	FYI	2.19	n/a	0.01	0.02	n/a
28 May 2015	3	Main coring site	SYI	1.55	n/a	0.17	0.18	n/a
28 May 2015	3	Secondary site	FYI	1.37	n/a	0.03	0.03	n/a
4 Jun 2015	3	Main coring site	SYI	1.62	n/a	0.16	0.17	n/a
5 Jun 2015	3	Secondary site	FYI	2.10	n/a	0.00	0.01	n/a
11 Jun 2015	4	Site1	FYI	1.74	n/a	0.00	0.00	n/a
13 Jun 2015	4	Site2	FYI	2.07	n/a	0.13	0.15	n/a
15 Jun 2015	4	Site3	FYI	2.19	n/a	0.00	0.00	n/a
17 Jun 2015	4	Site2	FYI	2.05	n/a	0.09	0.10	n/a
21 Jun 2015	4	Floe NB 1	FYI	1.93	n/a	0.05	0.06	n/a
21 Jun 2015	4	Floe NB 2	FYI	2.19	n/a	0.00	0.00	n/a

[a]The ice type is based on evaluation of the $\delta^{18}O$ and salinity profiles (see text).
[b]Note ice cores with structure analyses (see Table 1 and supporting information Figures S1–S5); n/a = not available.

$\delta^{18}O$ values of $+2.0$–$2.3‰$ in the bottom parts of SYI and FYI cores (e.g., Figure 3b) fit well into the assumption that $\delta^{18}O$ fractionation during columnar sea ice growth ranges naturally between $+1.5$ and $+2.6‰$ [cf. *McDonald et al.*, 1995; *Toyota et al.*, 2013]. Fractionation is higher for slower growth rates [*Toyota et al.*, 2013], as would have been the case for the bottommost parts, especially when the ice was often covered by rather thick snow to further slow ice growth [*Sturm and Massom*, 2010]. This layering and the properties combined suggest that this ice is likely to be SYI (or older), with the upper layer originating in the Laptev Sea and that it has been desalinated during summer. In the Laptev Sea, surface waters have a lower salinity and $\delta^{18}O$ values [e.g., *Bauch et al.*, 2012] than in the region north of Svalbard.

Based on the above, the ice cores collected during N-ICE2015 were either classified as FYI or SYI (Table 2), and this is also supported by an analysis of sea ice back trajectories which place the origin of the oldest ice of the ice pack in the N-ICE2015 study region to the Laptev Sea region in fall 2013 [*Itkin et al.,* 2017]. Floes 1, 2, and 3 were likely composed of a composite of FYI and SYI floes frozen together, while on Floe 4 we only found FYI-type ice cores (Table 1). On average, the bulk salinity of ice cores identified as FYI (4.9), was significantly higher than the value of 2.7 for SYI (Table 1). Note that despite the fact that the ice warmed up in June, the salinity is still relatively high for the FYI cores from Floe 4 (Table 1).

While in the majority of ice cores the $\delta^{18}O$ values of surface layers were in between the value for seawater and snow (Figure 3b), in a few ice cores surface layer $\delta^{18}O$ values approached that of snow (Figures 2b and 3a). For example, in the ice core collected for structural analyses on 26 January (Figure 2), the uppermost granular layer had larger crystals than the granular ice below. These layers also had low salinity (<0.3). This is indicative of superimposed ice [*Kawamura et al.*, 2001a]. These superimposed ice layers apparently survived a summer of surface melt.

3.2. Snow Fraction by Mass

For cores with only salinity and $\delta^{18}O$ profile data (e.g., Figure 3), we assume that layers with relatively constant values in the bottom half of the ice cores were formed during congelation growth, and thus represent fractionation during seawater freezing. The $\delta^{18}O$ values of these layers are used as the reference value δ_{boti}

for ice cores without structural information where the columnar ice layers can be defined unambiguously (Table 2). As noted above, Figure 3a shows an example of what appears to be a second-year ice core, with two layers with relatively constant salinity and $\delta^{18}O$ values with depth, below a surface layer with lower $\delta^{18}O$ values, thus the value for the upper of these two layers is should be used as the δ_{boti} value.

The fraction of snow by mass in the individual ice cores (F) varied from 0 to 18% when using δ_{sw} as reference and the mean δ_{snow} (Table 2). The snow contribution by mass for all cores, based on the *absolute* method after *Jeffries* [1997], and taking into account the variable δ_{snow} [cf. *Jeffries et al.*, 2001], was 7.5–9.7%. This compares reasonably well with observations from pack ice in the Sea of Okhotsk [*Ukita et al.*, 2000], and landfast ice in both a Svalbard fjord [*Nicolaus et al.*, 2003] and the Baltic Sea [*Uusikivi et al.*, 2011]. In the only study in the high-Arctic, on landfast sea ice in Baffin Bay, *Kawamura et al.* [2001b] found the snow contribution to be negligible. For Antarctic sea ice, snow fractions up to 14–16% have been reported [*Jeffries et al.*, 1997], although values typically range between 3 and 8% [e.g., *Lange et al.*, 1990; *Eicken et al.*, 1995; *Jeffries et al.*, 1994, 2001].

Both FYI and SYI cores had contributions from snow, but in SYI it was considerably higher, with an average F_{sw} of 12.7–16.3% versus 3.3–4.4% (using the *absolute* method), respectively. Higher snow contribution in SYI can be caused by several mechanisms, for example, snow fall early on in the second growth season when the ice is thin and when a thin snow cover may result in flooding [*Sturm and Massom*, 2010]. It appears that snow-ice formation was the governing mechanism for snow incorporation into sea ice. This again could be explained by the fact that surface ablation in summer could erode away superimposed ice, as it commonly forms before the primary summer melt period. Superimposed ice is likely often a transient feature in the sea ice mass balance in the Arctic [cf. *Nicolaus et al.*, 2003; *Granskog et al.*, 2006]. The increased amount of surface ablation in recent years [*Perovich et al.*, 2014] could likely melt away much of superimposed ice formed in spring and summer, even if all snow was converted into superimposed ice. Although in some years, however, surface ablation can be minimal [*Haas and Eicken*, 2001] and superimposed ice can survive the summer melt. This seems to be the case in a few of our ice cores, with surface layer of low salinity and $\delta^{18}O$ values as low as snow (supporting information Figures S1 and S3). In FYI, we would not expect any superimposed ice to have formed at the time of our sampling. However, the cores sampled in late June all had snow-ice layers. Thus, superimposed ice layers found in winter ice cores are also an indication of ice that is SYI or older, since our ice cores were sampled prior to any snow melt had occurred.

4. Conclusions

We have provided the first analyses of the snow contribution to sea ice mass balance from ice cores collected in the central Arctic pack ice, where a relatively thin and heavily snow-covered ice pack prevailed north of Svalbard in winter and spring 2015. The aim of the N-ICE2015 campaign was to understand the new thinner sea ice regime in the Arctic Ocean [*Granskog et al.*, 2016].

In concert with our observations, several ice mass balance buoys were deployed during the N-ICE2015 campaign. In winter, a number of these IMBs recorded rapid flooding [*Provost et al.*, 2017], associated with storms and ice breakup events and after basal melt near the ice edge far away from where majority of our ice cores were collected. Both for floe break up and basal ice melt, readjustment of isostacy likely lead to rapid flooding and the potential for snow-ice formation, which resembles the observations right at the ice edge further south in Fram Strait by *Tucker et al.* [1991]. Our ice cores, on the other hand, record snow that had been incorporated into the sea ice cover earlier in the growth season(s) and within the pack ice away from the ice edge. This shows that snow incorporation does not only occur in the marginal ice zone as reported by *Tucker et al.* [1991] and *Provost et al.* [2017].

In summary, we have shown that snow contributes to the mass balance of thinner first-year and second-year sea ice north of Svalbard. Any indication in the growth processes involved based on sea ice structure is precluded due to the small number of cores we have analyzed. Based on our analyses of 29 sea ice cores, snow contributes on average 7.5–9.7% to the sea ice mass. In second-year ice, the snow contribution is significantly higher (12.7–16.3%) than in first-year sea ice (3.3–4.4%). The salinity of first-year ice (4.9) is higher than that of second-year ice (2.7), not surprising given the desalination during the summer melt. Snow was largely incorporated as snow-ice, although a few cores with superimposed ice were evident in second-year ice cores based on the isotopic signatures. Thus, some superimposed ice appears to have survived summer

melt. One could in our case use the salinity and isotopic data to infer whether the ice is first-year ice or second-year ice (or older). Given the trends for more seasonal and much thinner ice in the Arctic basin, the potential for increasing contribution of snow to the Arctic sea ice mass balance is evident, thus an "antarctification" of the Arctic sea ice pack is likely. However, there is a delicate balance between an increase to the sea ice mass and a decrease in thermodynamic growth [e.g., *Leppäranta*, 1983]. The timing and fate of snow fall will be critical in determining the overall effect of the snow cover to Arctic sea ice mass balance when the ice gets thinner [cf. *Hezel et al.*, 2013]. Due to lack of data, we recommend further studies on snow contribution to Arctic sea ice mass balance, in different regions of the Arctic as regional differences may exist. Critically, more snow depth data are needed on Arctic sea ice.

References

Bauch, D., J. A. Hölemann, I. A. Dmitrenko, M. A. Janout, A. Nikulina, S. A. Kirillov, T. Krumpen, H. Kassens, and L. Timokhov (2012), Impact of Siberian coastal polynyas on shelf-derived Arctic Ocean halocline waters, *J. Geophys. Res.*, *117*, C00G12, doi:10.1029/2011JC007282.

Bintanja, R., and F. M. Selten (2014), Future increases in Arctic precipitation linked to local evaporation and sea-ice retreat, *Nature*, *509*(7501), 479–482, doi:10.1038/nature13259.

Cavalieri, D. J., C. L. Parkinson, P. Gloersen, and H. J. Zwally. (1996), Sea Ice Concentrations from Nimbus-7 SMMR and DMSP SSM/I-SSMIS Passive Microwave Data, Version 1, NASA Natl. Snow and Ice Data Cent., Boulder, Colo.

Dodd, P. A., B. Rabe, E. Hansen, E. Falck, A. Mackensen, E. Rohling, C. Stedmon, and S. Kristiansen (2012), The freshwater composition of the Fram Strait outflow derived from a decade of tracer measurements, *J. Geophys. Res.*, *117*, C11005, doi:10.1029/2012JC008011.

Eicken, H. (1998), Deriving modes and rates of ice growth in the Weddell Sea from microstructural, salinity and stable-isotope data, in *Antarctic Sea Ice: Physical Processes, Interactions and Variability, Antarctic Res. Ser.*, vol. 74, edited by M. O. Jeffries, pp. 89–122, AGU, Washington, D. C.

Eicken, H., M. A. Lange, H.-W. Hubberten, and P. Wadhams (1994), Characteristics and distribution patterns of snow and meteoric ice in the Weddell Sea and their contribution to the mass balance of sea ice, *Ann. Geophys.*, *12*(1), 80–93.

Eicken, H., M. Lensu, M. Leppäranta, W. B. Tucker, A. J. Gow, and O. Salmela (1995), Thickness, structure, and properties of level summer multiyear ice in the Eurasian sector of the Arctic Ocean, *J. Geophys. Res.*, *100*, 22,697-22,710.

Fichefet, T., and M. Maqueda (1999), Modelling the influence of snow accumulation and snow-ice formation on the seasonal cycle of the Antarctic sea-ice cover, *Clim. Dyn.*, *15*, 251–258, doi:10.1007/s003820050280.

Girard-Ardhuin, F., and R. Ezraty (2012), Enhanced Arctic sea ice drift estimation merging radiometer and scatterometer data, *IEEE Trans. Geosci. Remote Sens.*, *50*, 2639–2648.

Granskog, M., P. Assmy, S. Gerland, G. Spreen, H. Steen, and L. H. Smedsrud (2016), Arctic research on thin ice—Consequences of Arctic sea ice loss, *Eos Trans. AGU*, *97*(5), 22–26, doi:10.1029/2016EO044097.

Granskog, M. A., T. A. Martma, and R. A. Vaikmäe (2003), Development, structure and composition of land-fast sea ice in the northern Baltic Sea, *J. Glaciol.*, *49*(164), 139–148.

Granskog, M. A., M. Leppäranta, T. Kawamura, J. Ehn, and K. Shirasawa (2004), Seasonal development of the properties and composition of landfast sea ice in the Gulf of Finland, the Baltic Sea, *J. Geophys. Res.*, *109*, C02020, doi:10.1029/2003JC001874.

Granskog, M. A., T. Vihma, R. Pirazzini, and B. Cheng (2006), Superimposed ice formation and surface energy fluxes on sea ice during the spring melt–freeze period in the Baltic Sea, *J. Glaciol.*, *44*(176), 139–146, doi:10.3189/172756506781828971.

Haapala, J., M. Lensu, M. Dumont, A. H. H. Renner, M. A. Granskog, and S. Gerland (2013), Small-scale horizontal variability of snow, sea-ice thickness and freeboard in the first-year ice region north of Svalbard, *Ann. Glaciol.*, *54*(62), 261–266, doi:10.3189/2013AoG62A157.

Haas, C., and H. Eicken (2001), Interannual variability of summer sea ice thickness in the Siberian and central Arctic under different atmospheric circulation regimes, *J. Geophys. Res.*, *106*, 4449–4462.

Haas, C., D. N. Thomas, and J. Bareiss (2001), Surface properties and processes of perennial Antarctic sea ice in summer, *J. Glaciol.*, *47*(159), 613–625.

Hezel, P. J., X. Zhang, C. M. Bitz, B. P. Kelly, and F. Massonnet (2013), Projected decline in spring snow depth on Arctic sea ice caused by progressively later autumn open ocean freeze-up this century, *Geophys. Res. Lett.*, *39*, L17505, doi:10.1029/2012GL052794.

Itkin, P., G. Spreen, M. Doble, F. Ardhuin, B. Cheng, J. Haapala, S. Hudson, N. Hughes, L. Kaleschke, M. Nicolaus, and J. Wilkinson (2017), Thin ice and storms: a case study of sea ice deformation from buoy arrays deployed during N-ICE2015, *J. Geophys. Res. Oceans.*, doi:10.1002/2016JC012403.

Jeffries, M. O. (1997), Describing the composition of sea-ice cores and the development of the Antarctic sea-ice cover, *Antarct. J. U. S.*, *32*(5), 55–56.

Jeffries, M. O., R. A. Shaw, K. Morris, A. L. Veazey, and H. R. Krouse (1994), Crystal structure, stable isotopes (δ^{18}O), and development of sea ice in the Ross, Amundsen, and Bellingshausen seas, Antarctica, *J. Geophys. Res.*, *99*, 985–995.

Jeffries, M. O., A. P. Worby, K. Morris, and W. F. Weeks (1997), Seasonal variations in the properties and structural composition of sea ice and snow cover in the Bellingshausen and Amundsen Seas, Antarctica, *J. Glaciol.*, *43*(143), 138–151.

Jeffries, M. O., H. Roy Krouse, B. Hurst-Cushing, and T. Maksym (2001), Snow-ice accretion and snow-cover depletion on Antarctic first-year sea-ice floes, *Ann. Glaciol.*, *33*(1), 51–60.

Kawamura, T., K. I. Ohshima, T. Takizawa, and S. Ushio (1997), Physical, structural and isotopic characteristics and growth processes of fast sea ice in Lutzow Holm Bay, Antarctica, *J.Geophys. Res.*, *102*, 3345–3355.

Kawamura, T., K. Shirasawa, N. Ishikawa, A. Lindfors, K. Rasmus, M. A. Granskog, J. Ehn, M. Leppäranta, T. Martma, and R. Vaikmäe (2001a), Time-series observations of the structure and properties of brackish ice in the Gulf of Finland, *Ann. Glaciol.*, *33*, 1–4, doi:10.3189/172756401781818950.

Kawamura, T., K. Shirasawa, and K. Kobinata (2001b), Physical properties and isotopic characteristics of landfast sea ice around the North Water (NOW) Polynya region, *Atmos.-Ocean*, *39*(3), 173–182, doi:10.1080/07055900.2001.9649674.

King, J., S. Gerland, G. Spreen, and M. Bratrein (2016), *N-ICE2015 sea-ice thickness measurements from helicopter-borne electromagnetic induction sounding*, Norw. Polar Inst., Tromsø, Norway, doi:10.21334/npolar.2016.aa3a5232.

Kurtz, N. T., and S. L. Farrell (2011), Large-scale surveys of snow depth on Arctic sea ice from Operation IceBridge, *Geophys. Res. Lett.*, *38*, L20505, doi:10.1029/2011GL049216.

Lange, M. A. (1988), Basic properties of antarctic sea ice as revealed by textural analysis of ice cores, *Ann. Glaciol.*, *10*, 95–101.

Lange, M. A., P. Schlosser, S. F. Ackley, P. Wadhams, and G. S. Dieckmann (1990), ^{18}O concentrations in sea ice of the Weddell Sea, Antarctica, *J. Glaciol.*, *36*(124), 315–323.

Leppäranta, M. (1983), A growth model for black ice, snow ice and snow thickness in subarctic basins, *Hydrol. Res.*, *14*(2), 59–70.

Lindsay, R., and A. Schweiger (2015), Arctic sea ice thickness loss determined using subsurface, aircraft, and satellite observations, *Cryosphere*, *9*, 269–283, doi:10.5194/tc-9-269-2015.

Macdonald, R. W., D. W. Paton, E. C. Carmack, and A. Omstedt (1995), The freshwater budget and under-ice spreading of Mackenzie River water in the Canadian Beaufort Sea based on salinity and 18O/16O measurements in water and ice, *J. Geophys. Res.*, *100*, 895–919, doi: 10.1029/94JC02700.

Massom, R. A., et al. (2001), Snow on Antarctic sea ice, *Rev. Geophys.*, *39*, 413–445, doi:10.1029/2000RG000085.

Meier, W. N., et al. (2014), Arctic sea ice in transformation: A review of recent observed changes and impacts on biology and human activity, *Rev. Geophys.*, *52*, 185–217, doi:10.1002/2013RG000431.

Melnikov, I. A., and V. I. Lobyshev (1985), Fractionation of ^{18}O in the snow and ice of the central Arctic Basin, *Oceanology*, *25*(2), 181–184.

Nicolaus, M., C. Haas, and J. Bareiss (2003), Observations of superimposed ice formation at melt-onset on fast ice on Kongsfjorden, Svalbard, *Phys. Chem. Earth*, *28*, 1241–1248, doi:10.1016/j.pce.2003.08.048.

Nomura, D., P. Assmy, G. Nehrke, M. A. Granskog, M. Fischer, G. S. Dieckmann, A. Fransson, Y. Hu, and B. Schnetger (2013), Characterization of ikaite (CaCO3•6H2O) crystals in first-year Arctic sea ice north of Svalbard, *Ann. Glaciol.*, *54*(62), 125–131, doi:10.3189/2013AoG62A034.

Perovich, D., J. Richter-Menge, C. Polashenski, B. Elder, T. Arbetter, and O. Brennick (2014), Sea ice mass balance observations from the North Pole Environmental Observatory, *Geophys. Res. Lett.*, *41*, 2019–2025, doi:10.1002/2014GL059356.

Perovich, D. K., T. C. Grenfell, B. Light, B. C. Elder, J. Harbeck, C. Polashenski, W. B. Tucker, and C. Stelmach (2009), Transpolar observations of the morphological properties of Arctic sea ice, *J. Geophys. Res.*, *114*, C00A04, doi:10.1029/2008JC004892.

Provost, C., N. Sennéchael, J. Miguet, P. Itkin, A. Rösel, Z. Koenig, N. Villacieros, and M. A. Granskog (2017), Observations of snow-ice formation in a thinner Arctic sea ice regime during the N-ICE2015 campaign: Influence of basal ice melt and storms, *J. Geophys. Res. Oceans.*, doi:10.1002/2016JC012011.

Rösel, A., et al. (2016a), N-ICE2015 snow depth data with Magna Probe, Norw. Polar Inst., Tromsø, Norway, doi:10.21334/npolar.2016.3d72756d.

Rösel, A., et al. (2016b), N-ICE2015 total (snow and ice) thickness data from EM31, Norw. Polar Inst., Tromsø, Norway, doi:10.21334/npolar. 2016.70352512.

Sturm, M., and R. Massom (2010), Snow on sea ice, In *Sea Ice*, 2nd ed., edited by D. Thomas and G. Dieckmann, pp. 153–204, Wiley-Blackwell, Chichester, U. K.

Toyota, T., I. J. Smith, A. J. Gough, P. J. Langhorne, G. H. Leonard, R. J. Van Hale, A. R. Mahoney, and T. G. Haskell (2013), Oxygen isotope fractionation during the freezing of sea water, *J. Glaciol.*, *59*(216), 697–710, doi:10.3189/2013JoG12J163.

Tucker, W. B., T. C. Grenfell, R. G. Onstott, D. K. Perovich, A. J. Gow, R. A. Shuchman, and L. L. Sutherland (1991), Microwave and physical properties of sea ice in the winter marginal ice zone, *J. Geophys. Res.*, *96*, 4573–4587, doi:10.1029/90JC02269.

Tucker, W. B., III, A. J. Gow, D. A. Meese, H. W. Bosworth, and E. Reimnitz (1999), Physical characteristics of summer sea ice across the Arctic Ocean, *J. Geophys. Res.*, *104*, 1489–1504, doi:10.1029/98JC02607.

Ukita, J., T. Kawamura, N. Tanaka, T. Toyota, and M. Wakatsuchi (2000), Physical and stable isotopic properties and growth processes of sea ice collected in the southern Sea of Okhotsk, *J. Geophys. Res.*, *105*, 22,083–22,093, doi:10.1029/1999JC000013.

Uusikivi, J., M. A. Granskog, and E. Sonninen (2011), Meteoric ice contribution and influence of weather on landfast ice growth in the Gulf of Finland, Baltic Sea, *Ann. Glaciol.*, *52*(57), 91–96. doi:10.3189/172756411795931796

Warren, S. G., I. G. Rigor, N. Untersteiner, V. F. Radionov, N. N. Bryazgin, Y. I. Aleksandrov, and R. Colony (1999), Snow depth on Arctic sea ice, *J. Clim.*, *12*(6), 1814–1829, doi:10.1175/1520-0442(1999)012<1814:SDOASI>2.0.CO;2.

Webster, M. A., I. G. Rigor, S. V. Nghiem, N. T. Kurtz, S. L. Farrell, D. K. Perovich, and M. Sturm (2014), Interdecadal changes in snow depth on Arctic sea ice, *J. Geophys. Res. Oceans*, *119*, 5395–5406, doi:10.1002/2014JC009985.